Comparative Medicine
Copyright 2001
by the American Association for Laboratory Animal Science

Vol 51, No 4
August 2001
Pages 341-348

The Pig as a Model for Excisional Skin Wound Healing: Characterization of the Molecular and Cellular Biology, and Bacteriology of the Healing Process

Jian Fei Wang, DVM,[1,2] Merle E. Olson, DVM,[1,2] Carol R. Reno,[1] J. Barry Wright, PhD,[1,3] and David A. Hart, PhD[1]*

A pig model of wound healing was developed by excision of 2-cm-diameter full thickness skin in young Yorkshire pigs. The results indicated that wound re-epithelialization in this animal model took an average of 20 days. Analysis of cellular change was assessed by use of DNA quantification and determination of apoptotic cells in tissue sections. The results indicate that RNA and DNA contents paralleled each other throughout the healing process, and observed changes in the pattern of RNA and DNA content of the scar tissues were consistent with cell loss due to apoptosis in this model. Expression of mRNA for relevant genes was assessed by use of semiquantitative reverse transcription-polymerase chain reaction (RT-PCR) analysis, using porcine specific primer sets and RNA isolated from normal skin and specimens obtained at various times after wounding. The mRNA values for tumor necrosis factor-α (TNF-α), connective tissue growth factor (CTGF), insulin-like growth factor II (IGF-II), and decorin were significantly high at specific times after wounding, but mRNA values for the transcription factors (c-fos and c-jun) were significantly decreased. Quantitative bacteriologic results indicated that the total bacterial count in this animal model reached 10^9 colony-forming units (CFU)/g, with the highest value at post-wounding day 7, and *Pseudomonas aeruginosa* and *Staphylococcci aureus* were the most common bacteria detected in this model. Further definition of this model should identify unique points in the healing process, and such information could lead to development of therapeutic interventions to improve skin wound healing.

In a normal individual, when skin is disrupted, a series of interdependent physiologic events, including inflammation, re-epithelialization, angiogenesis, granulation tissue formation, and extracellular matrix remodeling, occur that result in tissue repair through formation of scar tissue (1). Over the past two decades, extraordinary effort has been made to investigate the molecular and cell biology of skin wound healing. The goal of such studies is to understand the healing process to improve the outcome for patients with defective healing potential (the elderly, diabetics, those on certain drugs), as well as those with excess healing responses (keloid and hypertrophic scar formation).

In skin wounds, another complication of the healing process is infection. Infection of skin wounds with organisms such as *Staphylococcus* and *Pseudomonas* spp. is a common clinical problem that can lead to alterations in wound healing, as well as increases in morbidity and mortality of infected patients. Therefore, better understanding of wound molecular and cellular biology and bacteriology will definitely aid in new therapeutic development, and in turn, improve wound healing.

Investigation of the biology of wound healing has long depended on use of various animal models because they provide a means of studying the complex interactions that occur in living tissue without the limitations and artifacts inherent to use of in vitro techniques (2). Currently, most researchers use rodent models in wound-healing studies because of their low cost, small size, and relative ease of handling and care. The rodent healing response is similar to that in humans, with collagen deposition leading to scar formation. However, the fact that keloids, hypertrophic scar formation, and intra-abdominal adhesions do not develop, indicates that healing in such animals is not identical to human wound healing (2). Although primates are phylogenetically close to humans, they differ from humans in that exuberant scar formation is not characteristic of their healing response (2).

Pigs are well accepted as being one of the best models of human dermal repair due to the similarities between porcine and human skin (3). These similarities include relative thickness of the dermis and epidermis and presence of a similar density of dermal appendages (3). Juvenile domestic pigs are usually used because they are small in size, making them comparably easy to handle and house. Although wounds in a young animal tend to heal quickly, the healing process proceeds over a few weeks, which is sufficient to assess temporal aspects of the molecular and cellular biology of the healing process.

In the study reported here, we continue to characterize a pig model for the study of open wound healing, and extend our previous observations (4, 5). Using full-thickness wounds, we assessed bacteriology during the healing process and used semiquantitative reverse transcriptase-polymerase chain reaction (RT-PCR) analysis to expand the evaluation the mRNA content for several important molecules in this model during the healing process, as well as define the cellular biology of the maturing scar tissue. The results indicate this model is suitable for the study of therapeutic interventions to improve skin

Received: 4/24/01. Revision requested: 4/30/01. Accepted: 7/17/01.
[1]McCaig Center for Joint Injury and Arthritis Research, Department of Microbiology and Infectious Disease, Faculty of Medicine, [2]Animal Resource Center, University of Calgary, 3330 Hospital Drive, North West, Calgary, Alberta, Canada T2N 4N1, and [3]Westaim Biomedical Corp., Fort Saskatchewan, Alberta, Canada.
**Corresponding author.*

wound healing, as well as define deficiencies in wound healing induced by secondary disease or genetics.

Materials and Methods

Animals and animal care. For this study, 32 Yorkshire pigs ([15 to 20 kg] Siva Farms, Calgary, Alberta, Canada) raised under specific-pathogen-free condition(s) (6) were used, including tissue and RNA from 7 animals used in previous studies (4). The animals were housed individually in 1.6 × 2-m suspended steel cages at the University of Calgary Animal Resource Center with a 12-h light/dark cycle. The animals were fed antibiotic-free food (Unifeed Ltd., Calgary, Alberta, Canada) and water ad libitum and were housed and maintained in accordance with Canadian Council of Animal Care guidelines.

Animal model. Wound induction has been described (5). Briefly, prior to wounding, animals were sedated by intramuscular administration of a mixture of ketamine (10 mg/kg of body weight: Ketalean, MTC Pharmaceuticals, Cambridge, Ontario, Canada) and acepromazine (0.2 mg/kg: Atravet, Ayerst Laboratories, Guelph, Ontario, Canada), followed by complete general anesthesia induced by mask inhalation of 1 to 2 % halothane (MTC Pharmaceuticals, Cambridge, Ontario, Canada). After induction of anesthesia, hair over the dorsum of the animals was clipped, using a No. 40 Osler blade and the skin was subsequently scrubbed with a non-antibiotic-containing soap. Each animal was reproducibly subjected to full-thickness skin wounds by use of a trephine. Before wounding, normal skin specimens in each location were collected by use of a 4-mm-diameter biopsy punch. On each animal, twenty 2-cm-diameter wounds were created on the back. The wounds were spaced a minimum of two cm apart and were created in four columns parallel to the dorsal midline, two columns on each side of dorsal thoracolumbar midline (5). Saline/epinephrine solutions were applied to the wound site until hemostasis was complete. The dressing materials were tripartite bandages composed of absorbent rayon/polyester cores, sandwiched between layers of non-adherent high-density polyethylene mesh. Each layer was spot-welded together and supplied sterilized and packaged (Westaim Biomedical Corp., Fort Saskatchewan, Alberta, Canada). The dressing was moistened in a tray of sterile water, drained, and applied to freshly created full-thickness dermal wounds. In all instances, the dressings were maintained moist by applying an occlusive surgical drape over the dressings. The dressings and drapes were held in place by use of Elastoplast. The dressings were changed three times per week after wounding; wound measurements were taken when dressings were changed. Specimens were taken from one or two wounds on each side of on each pig, using a 4-mm-diameter punch at designated times. Animals received a narcotic analgesic (butorphenol, Torbugesic, Ayerst Laboratories, 0.2 mg/kg) for pain management during surgical recovery and after sampling of wound sites.

Wound bacteriologic examination. On the day of surgery, several wounds were sampled to determine the initial degree of wound contamination. Thereafter, wounds were sampled on postsurgical days 1, 4, 7, 14, and 21. Quantitative biopsy specimens were aseptically acquired, using a sterile 4-mm trephine. The recovered tissue was placed in a preweighed, sterile tube, and wet weight of the tissue was determined. After determination of tissue weight, the tissue was macerated and subsequently serially diluted in phosphate-buffered saline (PBS; pH 7.0). The dilutions were plated on mannitol salts-containing agar (Difco, Detroit, Mich.), *Pseudomonas* isolation agar (Difco), and Mueller-Hinton agar (Difco) for recovery of staphylococci, pseudomonad s, and total bacteria, respectively. After growth and enumeration of the bacterial colonies, the number of colony-forming units per gram of wet weight of tissue was calculated.

Wound molecular biology. (i) RNA and DNA quantification. Total RNA was extracted from individual tissue specimens, using the TRIspin method (7) as described (4). The extracted total RNA was quantified fluorometrically, using the SYBR Green II fluorescent RNA dye (Molecular Probes, Inc., Eugene, Oreg.) and an LS-5 fluorescence spectrofluorometer (Perkin-Elmer, Foster City, Calif.) with excitation at 468 nm and emission at 525 nm. Standard RNA curves were established by use of rRNA (Sigma Chemical Co., St. Louis, Mo.) (8).

The DNA content was quantified fluorometrically essentially as described by Lipman (9). Standards made with calf thymus DNA were prepared similarly as those that had been prepared for each tissue specimen. Fluorescence was measured by use of a fluorometer (Model MPF-44B, Perkin-Elmer), with excitation and emission wavelengths of 350 and 450 nm, respectively. Slit widths were 10 and 15 nm, respectively.

(ii) Primer development and semi-quantitative RT-PCR analysis. Porcine-specific primers were developed, using previously derived rabbit primers (10, 11), which were found to detect analogous porcine sequences, or were directly derived from Genbank or literature porcine sequences. Cloning and sequencing of amplicons from each porcine-specific primer set have been described (4). For some molecules, primers were derived from internal sequences of such amplicons to optimize PCR-mediated detection of porcine mRNA. For each primer set, the annealing temperature, buffer conditions, and number of PCR cycles were optimized to ensure that the PCR reaction was in the linear range of amplification (Table 1) and within the linear range of the image-analysis system (12). For sample analysis, 2 mg of total RNA from each sample was reverse transcribed, using a Stratagene RT-PCR kit (Stratagene, La Jolla, Calif.). Samples of total RNA isolated from normal skin, day 1, 2, 3, 7, 14, 21, 35, and 49 wound/scar tissue from pigs were processed at the same time to minimize variation. Samples were then assessed for glyceraldehyde phosphate dehydrogenase(GAPDH, a housekeeping gene), mRNA content (10, 12) and subsequently, the molecules of interest. Semi-quantitative RT-PCR and data analyses were performed as described (4).

(iii) Wound apoptosis. Specimens for analysis of apoptotic cells were obtained on the same day and in similar manner as those obtained for molecular biology analysis except that the biopsy specimen was placed in a solution of neutral-buffered 4% paraformadehyde fixative prior to embedding. Specimens were dehydrated in alcohol and xylene, then were oriented and embedded in paraffin. Sections (5 μm) of each sample were then prepared. Apoptotic cells were detected by use of the Apop Tag *In Situ* Apoptosis Detection kit (Intergen, New York, N.Y.) with fluorescence (13). Photographs of each section were taken for permanent records. The degree of apoptosis was estimated, using a qualitative scoring system that was based on the overall amount of apoptosis observed in the wound. The apoptosis scoring system was reported by Brown and co-workers (14). Scoring was performed by three separate observers blinded to specimen identity. Scores were then averaged to generate a final score. Separate observer scores never differed by more than one point. Zero was assigned for no apoptotic

Table 1. Polymerase chain reaction primers used in the study

Primer		Sequence	bp	Annealing temperature	Optimal cycle	Source
Collagen III	1	TTA TAA ACC AAC CTC TTC CT	255	55	32	Reference 10
	2	TAT TAT AGC ACC ATT GAG AC				
GAPDH	1	TCA CCA TCT TCC AGG AGC GA	293	55	29	Genbank accession No. L23961
	2	CAC AAT GCC GAA GTG GTC GT				
TNF-α	1	CAC TGA GAG CAT GAT CCG AG	463	60	36	Reference 38
	2	GGC TGA TGG TGT GAG TGA GG				
CTGF	1	GCT CTT CTT CAT GAC CTC ACC GT	411	60	32	Genbank accession No. U83916
	2	GCG GCT TAC CGA CTG GAA GAC AC				
Decorin	1	AAC TCT TCA GGA GCT GCG TG	456	60	29	Genbank accession No. AF125537
	2	GCC GAC TGC AGA GAT GTT GT				
IGF-II	1	GAC CGC GGC TTC TCA TT	205	60	31	Reference 12
	2	GGA AGA ACT TGC CCA CG				
c-fos	1	ACC AGC CCA GAC CTG CAG TGG	261	65	31	Reference 11
	2	CCG GCA CTT GGC TGC AGC CAT				
c-jun	1	CCC CTG TCC CCC ATC GAC ATG	267	55	38	Reference 11
	2	TTG CAA CTG CTG CGT TAG CAT				

1 = forward primer; 2 = reverse primer.
bp = base pairs; GADPH = glyceraldehyde phosphate dehydrogenase; TNF = tumor necrosis factor; CTGF = connective tissue growth factor; IGF= insulin-like growth factor.

cells, 1 for minimal, 2 for few, 3 for moderate, 4 for heavy, and 5 for maximal number of apoptotic cells.

(iv) Statistical analysis. Statistical analysis of the densitometric data comparing results for normal skin and for scar tissue was performed, using analysis of variance (ANOVA) and Excel 7.0 software. Significance was set at $P < 0.05$.

Results

Wound closure. To monitor wound re-epithelialization, measurement of wound size was taken at the time of wounding and at specific intervals post-wounding using established methods (15). There was some distortion of the wounds as healing progressed, so wound area was calculated, using the formula for the area of an ellipse (area = πab). The calculated wound areas were expressed as a percentage of the day-0 wound area. Fig. 1 shows that of the wounds had re-epithelialized by postinjury day 20.

Wound bacteriologic findings. Fig. 2 depicts the number of bacteria isolated from wound sites over the course of healing. The results indicate that the bacterial count was maximal between three and seven days after wounding (10^9 organisms/g of tissue). Subsequently, bacterial counts decreased and were maintained at 4×10^6 organisms/g of tissue till 21 days after wounding. By day 21, most of the bacteria detected were contained in microabcesses and were not surface organisms (data not shown). After plating of tissue extracts on selective media, it was determined that *P. aeruginosa* typically accounts for a large percentage of the bacteria in the wound isolates, with *S. aureus* also prevalent (Fig. 2). These findings are consistent with earlier results using this model (5).

Wound molecular biology. (i) Preliminary molecular studies. A total of 60 normal skin specimens (20/pig) were taken from various locations on the dorsum of three pigs and total RNA was extracted from each specimen. The RNA yields at the various locations on the pigs were compared. Fig. 3 shows no significant difference in RNA yield (micrograms per milligram wet weight) between the various pigs, or from various locations on the same pig. Furthermore, to test for variation in individual transcript levels between pigs, or from different locations, collagen III mRNA values for these 60 specimens (3 pigs, 20 samples/pig) were assessed. Fig. 4 shows no significant differences in mRNA values for collagen III between these 3 pigs, or between the various locations on each pig.

(ii) Changes in total RNA and DNA during wound healing. Fig. 5 shows the changes in total RNA and DNA per milligram wet weight of normal and scar tissues during wound healing in this model. Total RNA and DNA were observed to significantly increase 24 h after wounding, reaching a maximum by day 7 for both components. Subsequently, values gradually decreased over time, but scar tissue values were still significantly higher than normal skin values even at day 49 ($P = 0.015$ for RNA, $P = 0.004$ for DNA). It was noted that the change in total RNA and DNA during wound healing at different times is consistent and parallel. Therefore, any observed increase or decrease in specific mRNA values, as determined by semi-quantitative RT-PCR analysis, likely indicates per-cell alterations in gene expression.

(iii) Apoptosis during wound healing. In a previous study, wound histologic examination at various times after wounding was defined in the model (4). In the study reported here, this was extended to define cell apoptosis in wound tissue at various times after injury in the same model. Representative photographs of apoptotic cells in wounds at various times after wounding in this animal model are presented in Fig. 6. Only a very few apoptotic keratinocytes and fibroblasts were evident in normal skin. Apoptotic cells were observed one day after wounding, and a marked increase in apoptotic cells was evident by three days. After hematoxylin and eosin (H&E) staining of sections, these cells appeared to be inflammatory cells, with a predominance of polymorphonuclear neutrophilic leukocytes (PMNs) (4). A large percentage of apoptotic cells were observed at day seven; most cells were now fibroblastic in nature, as determined by H&E staining, and a few were inflammatory cells (4). By day 14, maximal percentages of apoptotic cells were detected and endothelial cells were now observed to be undergoing apoptosis. At day 21, the density of apoptotic cells was decreased, but a significant number of fibroblasts, endothelial cells, and keratinocytes were undergoing apoptosis. By day 35, a number of apoptotic cells were still evident, but by day 49, the density of apoptotic cells was much diminished. Fig. 7 shows the distribution of apoptotic cells that were scored in blinded manner by three independent observers, using the system of Brown and co-workers (14). Apoptotic cells underwent a time course that peaked at day 14 after wounding, then gradually decreased by day 49.

(iv) Decorin mRNA during wound healing. Decorin is a small non-aggregating proteoglycan that has been reported to

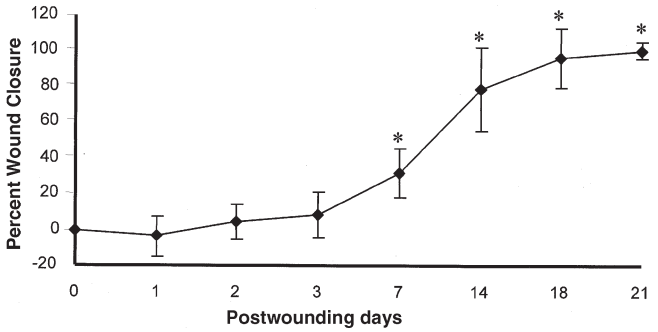

Figure 1. Kinetics of wound closure in the porcine model. Multiple 2-cm-diameter wounds were created on the dorsum of pigs at T = 0, and at the indicated times, the extent of wound closure was determined, using a digital calipers. For each time point, N = 4 pigs and 20 wounds/pig (total, 80 wounds). Values were presented as mean ± SEM, and values indicated by an asterisk (*) are significantly ($P < 0.05$) different from time-zero values.

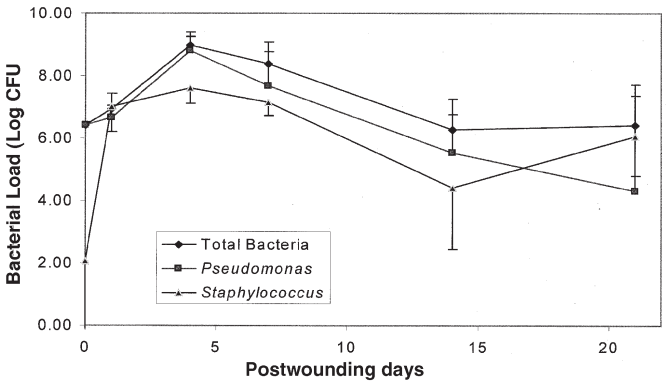

Figure 2. Bacterial quantification during healing of full-thickness wounds. Bacteria were isolated and quantified from tissues as described in the Materials and Methods section. Values are presented as mean ± SD (N = 56 at each time point).

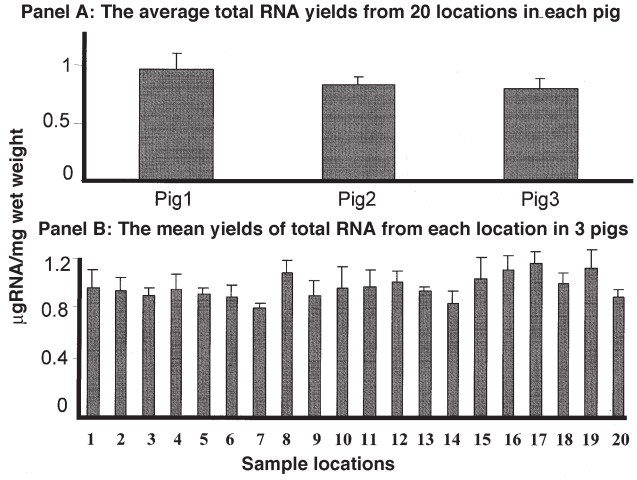

Figure 3. Analysis of total RNA content in skin from various locations on three pigs. Normal skin specimens from a total of 20 locations/pig, corresponding to the location of the wound sites, were taken as described in the Materials and Methods section. Positions 1-4 were the most cranial, and positions 17-20 were the most caudal locations. Panel A: values presented are the mean ± SEM total RNA yields per specimen per pig for these pigs. Panel B: values presented are mean ± SEM RNA yield at each location for three pigs.

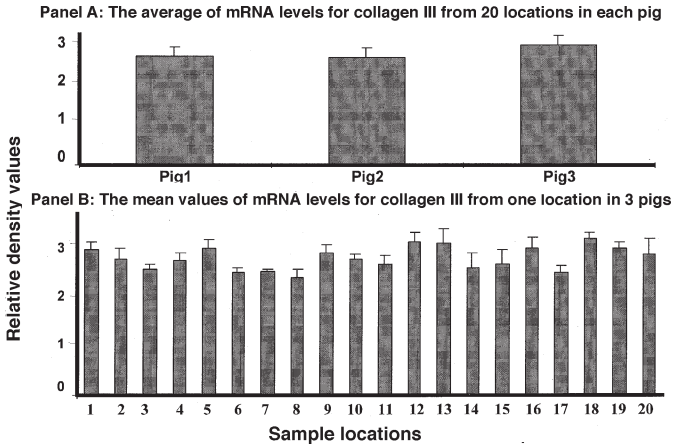

Figure 4. Quantification of mRNA levels for collagen III at various locations on three pigs. The RNA isolated from the 20 locations from each of three pigs (as described in the legend to Fig. 3) was assessed for collagen III mRNA levels, using semiquantitative reverse transcriptase-polymerase chain reaction (RT-PCR) analysis. Panel A: values presented are the mean ± SEM for the 20 locations on each pig. Panel B: values presented are the mean ± SEM at each location on three pigs.

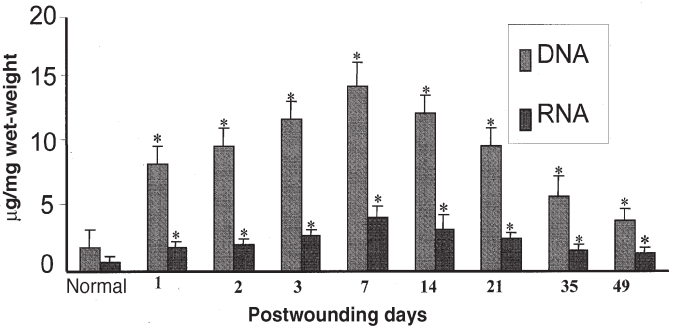

Figure 5. Comparison of total RNA and DNA from specimens taken at various times after wounding. At the indicated times after wounding, two specimens from four pigs were removed for RNA isolation and DNA assessment (N = 8 at each time point). Normal skin values were derived from skin taken at T = 0. Values are presented as mean ± SEM, and those indicated with an asterisk (*) are significantly different from normal values.

bind collagen and modulate collagen fibril formation (16). To determine whether mRNA levels for decorin were altered during skin wound healing, normal skin and wound specimens taken at various times after wounding were assessed by RT-PCR analysis. Fig. 8 (panel A) indicates that mRNA values for decorin were significantly increased by day seven after wounding, and thereafter, mRNA levels for this molecule progressively increasPed, reaching their highest value by day 35. Decorin mRNA levels then decreased, but were still significantly high at day 49, compared to normal tissue values (420% of normal).

(v) Tumor necrosis-α mRNA during wound healing. Tumor necrosis factor-α (TNF-α) is a mediator of the inflammatory response (17). The mRNA levels for TNF-α were assessed by RT-PCR analysis to determine whether expression of this molecule was altered during wound healing. As shown in Fig. 8 (panel B), a significant increase (780% of normal tissue values) in TNF-α mRNA levels were detected on day 1 after wounding ($P < 0.0001$). The TNF-α mRNA values remained significantly high at day 14 after wounding, compared with normal tissue values (180% of normal value, $P < 0.005$). Thereafter, TNF-α mRNA

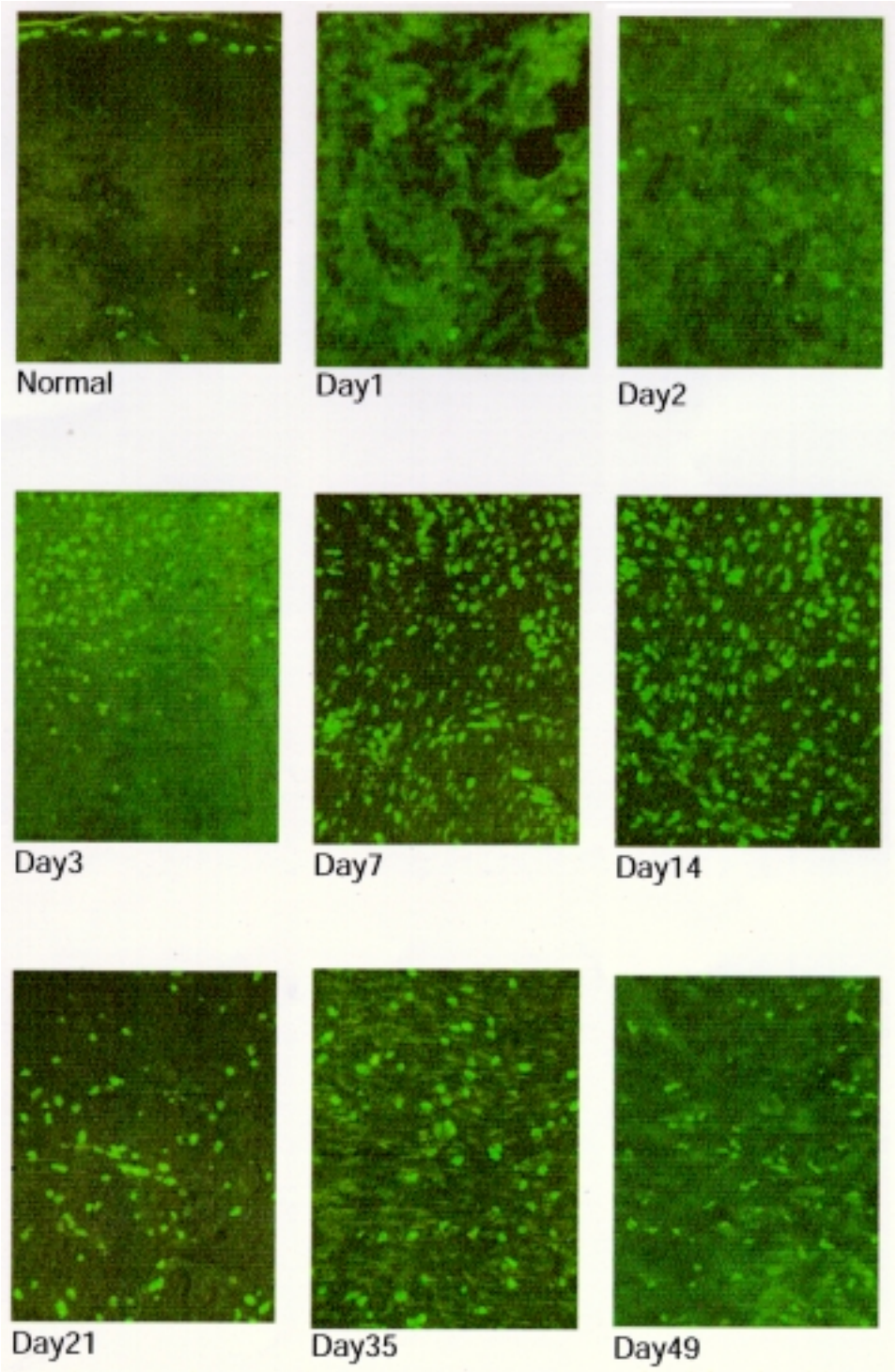

Figure 6. Apoptotic cells in normal skin and scar tissue at various times after wounding (×200). Paraffin sections of skin were assessed for apoptotic cells, using a commercial TUNEL assay as described in the Materials and Methods section.

values progressively decreased until they returned to near normal values by day 21.

(vi) Connective tissue growth factor (CTGF) mRNA during wound healing. Connective tissue growth factor has been reported to have an important role during wound healing by stimulating cell proliferation, cell adhesion, chemotaxis, angiogenesis, and production of extracellular matrix components (18). As shown in Fig. 8 (panel C), a significant ($P < 0.03$) increase in CTGF mRNA values up to 270% of normal tissue values was detected on day seven after wounding. The mRNA values for this growth factor then continued to increase and peaked on day 21 at 580% of normal values. Subsequently, mRNA values decreased, but were still significantly ($P = 0.01$) high at conclusion of the study (day 49).

(vii) Insulin-like growth factor II mRNA values during wound healing. Insulin-like growth factor II (IGF-II) is a growth factor that has diverse effects on metabolism and growth, and has been reported to have an active role in tissue repair in mice (19). To determine whether mRNA values for IGF-II were also altered in the porcine model during wound healing, normal tissue and wound specimens were assessed for this growth factor by use of RT-PCR analysis. Fig. 8 (panel D) shows that mRNA values for IGF-II were altered as wound healing progressed. The mRNA values for this growth factor were initially decreased, but were significantly high at day 14 in the healing response. The values reached maximum at day 35 ($P = 0.002$), then decreased. However, the values were still significantly high by day 49 ($P = 0.009$). Thus, mRNA values for CTGF and IGF-II were increased during wound healing, particularly during the later scar tissue remodeling stages.

(viii) Values of mRNA for c-fos and c-jun during wound healing. Two transcription factors, c-jun and c-fos, have been documented to have an important role in regulating expression of a number of genes, particularly at AP-1 sites (20). Therefore, mRNA values for c-jun and c-fos were also assessed during healing of skin wounds. Interestingly, mRNA values for c-jun and c-fos were significantly decreased during wound healing in this animal model from day one to day 35 (Fig. 9). However, values for both molecules returned to near normal by day 49 after wounding.

Discussion

As indicated by the results, this porcine animal model of wound healing provides a number of advantages. Young pigs are small, and easily handled and housed. Although wounds in young pigs tend to heal without complication, the healing process proceeds over a few weeks, which is sufficient to assess the bacteriology, as well as molecular and cellular biology of the healing process. As shown in Fig. 1, com-

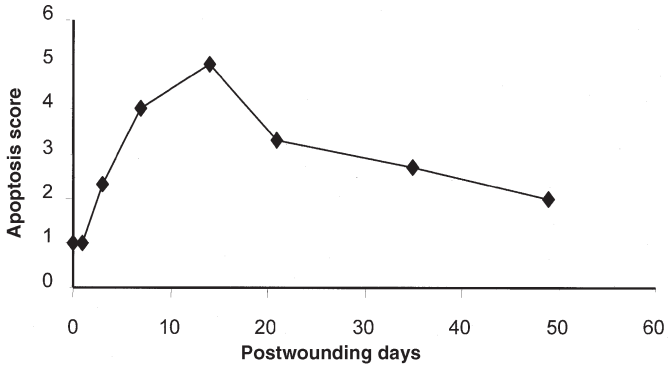

Figure 7. Apoptosis score during wound healing. Apoptotic cells in normal skin and healing wounds were assessed in tissue sections by three independent observers, as described by Brown and co-workers (14).

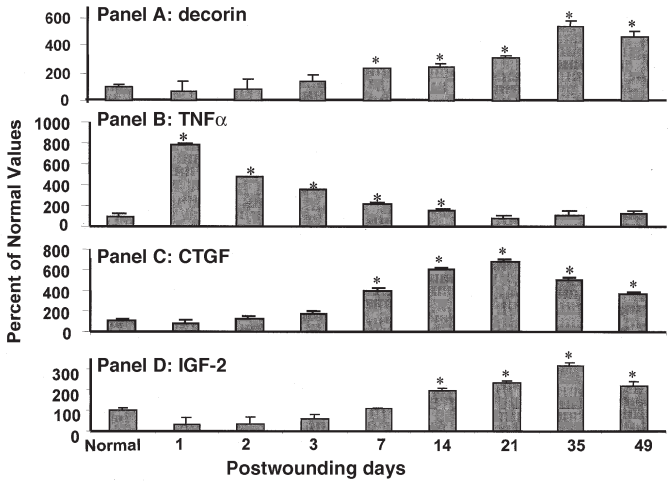

Figure 8. The mRNA levels for decorin (panel A), tumor necrosis factor-α (TNF-α; panel B), connective tissue growth factor (CTGF; panel C), and insulin-like growth factor II (IGF-II; panel D) during wound healing. The mRNA levels for each molecule were determined by use of semi-quantitative RT-PCR analysis, as described in the Materials and Methods section. The mean value for mRNA from normal skin was set at 100% and the mean ± SEM values from the various healing intervals is presented as percentage of the control values. All values indicated by * are significantly ($P < 0.05$, ANOVA) different from control values.

plete re-epithelialization in this model takes an average of 20 to 21 days, a time frame sufficient to use in evaluation of therapeutic interventions. Moreover, because the pig is considered a large animal, multiple, large wounds can be induced on a single animal and specimens from a single wound offer sufficient material for a variety of assessments. In contrast, due to the limitation of the wound size in rodents, a large number of animals are required to obtain the same results.

Many potential factors can influence wound healing (21). They include vascular insufficiency, prolonged inflammation, pressure necrosis, physical agents, cancer, and infection (22). Gross bacterial infection of wounds may certainly delay or even interfere with the healing response (23). Local destruction of tissue can result from extensive bacterial growth and enzymatic action, as well as prolongation of the inflammatory phase (2, 23). With emergence of antibiotic-resistant organisms such as methicillin-resistant *S. aureus*, the impact of infection on the healing process is becoming even more critical. *Pseudomonas*

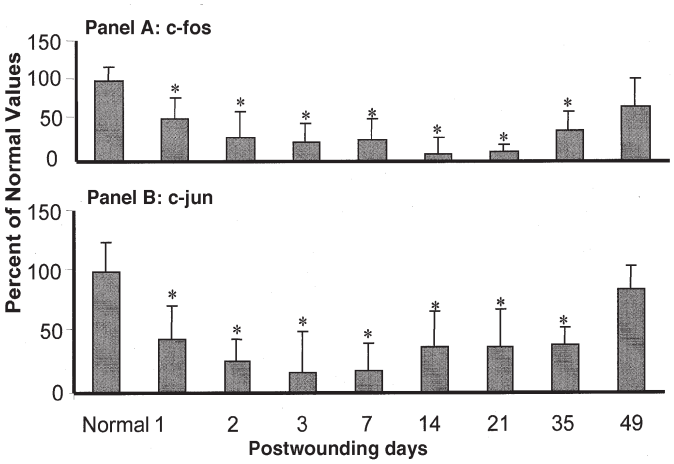

Figure 9. The mRNA levels for c-fos and c-jun during wound healing. Values for c-fos (panel A) and c-jun (panel B) were determined by use of semi-quantitative RT-PCR analysis, as described in the Materials and Methods section. *See* Figure 8 for key.

aeruginosa and *Staphylococcus aureus* were two prevalent organisms in those wounds. Thus, even when care is taken to prevent initial contamination of wound sites in this model, wounds become colonized with *P. aeruginosa* and *S. aureus* within a few days. In humans, staphylococci (10.5%) and pseudomonads (7.6%) are most frequently found in surgical wounds and cause a substantial percentage of hospital infections (24). *Staphylococcus aureus* is also reported to be a prominent organism in chronic wound infections (present in 62.9% of cases) (24). Therefore, this porcine model may mimic the clinically relevant condition, and will be useful for evaluating the impact of various antimicrobial therapies on wound healing in the future.

Assessment of total RNA (mRNA + rRNA + tRNA) from various locations on the dorsum indicated no significant difference in RNA yield (micrograms per milligram wet weight) from various pigs, or various locations in the same pig. In addition, assessment of mRNA levels for collagen III, an important extracellular matrix molecule, indicated no significant differences between different pigs, or between different locations in the same pig. Thus, these results indicate that multiple wound sites on a single animal can likely be used for long-term sequential assessment of wound healing.

Assessment of total RNA and DNA indicated that the total RNA values at each time point after wounding were closely paralleled by DNA values. The changes in total RNA and DNA during wound healing in this model likely paralleled fluctuations in the cellularity of the wound site. As the cellularity of the wound site appears to peak early, then decrease, either there is an efflux of cell from wounds or cells within wounds die. It is well known that there are two major mechanisms by which cells undergo death. Necrosis is the result of cellular damage that leads to lysis and release of intracellular contents. This process promotes inflammation (25) and would likely not be beneficial for healing. Programmed cell death or apoptosis provides a mechanism of autodigestion for specific cells that are no longer functioning properly or have outlived their usefulness (25).

The results indicated the presence of are rare apoptotic cells in normal skin. However, apoptotic cells were evident 24 h after wounding and greatly increased after 72 h, with most of them

likely being PMNs (4). The apoptotic cells reached a maximum by day 14, then decreased. However, by day 49, the number of apoptotic cells in scar tissue was still substantial. Histologic examination indicated that the apoptotic cells at day seven were principally fibroblasts; a few PMNs also were present. Whether the large number of PMNs in the early wound sites were there as part of the normal healing process or were there in part, due to the bacterial contamination/infection (Fig. 2) in the wounds must await further investigation. However, later in healing, most of apoptotic cells were fibroblasts and endothelial cells. By day 14, endothelial cells in the microvasculature were observed to undergo apoptosis. The numbers of apoptotic cells observed during the healing process in this pig model also are consistent with reported observations in a rat excisional full-thickness skin wound model (26). Thus, apoptosis is likely involved in mediating the decrease in cellularity during the progression of wound healing in both models. The decrease in total RNA and DNA content as the scar matures is consistent with cell loss due to apoptosis in this model (Fig. 5 and 6).

In this study, a number of molecular transcripts were assessed during wound healing. Although the number of molecules assessed in this study was not extensive, the breadth of the molecules assessed in this study, as well as those of a previously reported study (4), is sufficient to document that wound healing is a series of complex cell and matrix interactions. These data extended our baseline for molecular aspects of skin wound healing information in this animal model, and provide the basis to assess impaired or accelerated healing in this model at the molecular level in the future.

The finding that mRNA levels for TNF-α were high immediately after wounding indicates that this cytokine likely plays an important role in the inflammatory phase of tissue repair. Tumor necrosis factor-α is mainly produced by cells of the monocyte/macrophage lineage (27). It also has been reported to be a major angiogenic factor inducing capillary expansion into the wound area (28). In addition, TNF-α also is a strong initiator of inflammatory cascades (28). However, since infection can also lead to induction of TNF-α (29), and early wounds were infected, conclusions as to whether TNF-α induction occurred as a consequence of injury and/or infection must await further investigation.

Connective tissue growth factor, a cysteine-rich mitogenic peptide, has been reported to be involved in wound healing (30). This factor stimulates fibroblast cell growth, matrix production, and granulation tissue formation (31). In rats, CTGF expression peaked on day nine after injury and subsequent to peak expression of TGF-β on day three in the Schilling chamber model of wound repair (30). The co-coordinated expression of the two growth factors was interpreted to be regulated by components of a growth factor cascade in which TGF-β initiated regeneration and repair, and stimulated production of CTGF, which was required later in the wound healing process (18). Connective tissue growth factor has been reported to be a downstream mediator of TGF-β, and a TGF-β regulatory element in the CTGF promoter region has been identified (32).

Results of a previous study indicated that mRNA levels for TGF-β were modestly increased early (days one to three after wounding) after injury in this porcine model (4) and mRNA levels for collagen I and III were significantly increased by day seven (4). In the study reported here, mRNA levels for CTGF were significantly high later, possibly indicating that TGF-β and CTGF may also be part of a growth factor cascade that regulates aspects of wound healing in the pig model, similar to what was observed in the rat (30).

In incisional and subcutaneous sponge models of wounding, increased expression of IGF-II has been reported from one to 21 days after wounding in a mouse model (33). In our study, significant increases in IGF-II expression were detected by day 14. In fact, the increase in mRNA levels for IGF-II peaked after peak changes in CTGF. However, it remains to be determined whether there is a cause-and-effect relationship between the two growth factors, but the findings again were consistent with CTGF and IGF-II being part of a regulated growth factor cascade during the wound healing process

The time course for decorin expression during wound healing was delayed, compared with that of CTGF (Fig. 8), but was not unlike the pattern of change detected for IGF-II. In fact, the pattern change for expression of decorin mRNA levels even more closely paralleled those for collagen I and III (4). This small proteoglycan has been documented to bind collagens, particularly collagen I, and thus, modulates fibril formation (34). In addition, this proteoglycan can bind TGF-β and effectively make it unavailable for interaction with TGF-β receptors (35). The finding that decorin mRNA levels parallel those for other matrix molecules, and are still high at postwounding day 49, likely indicates that this molecule is involved in matrix remodeling of scar tissue rather than binding to TGF-β, which is high only very early in the healing process (4).

It was interesting to find that mRNA levels for c-fos and c-jun were significantly decreased during wound healing. It has been reported that these two transcription factors can be detected at the protein level in normal skin, early inflammatory cells, and later proliferative fibroblasts in human skin wounds at various postinjury intervals (36). In a study of human tissue, expression of c-jun and c-fos was not detected in normal skin, but protein and mRNA were detected for both transcription factors in dermal fibroblasts and elongated perivascular cells in keloid and hypertrophic scars (37). In our study, mRNA for c-fos and c-jun was clearly detected in normal skin, significantly decreased in early scar tissue (day 1–35 after injury); then values became more normalized by postwounding day 49. Whether the change in the pattern of these two transcription factors at the protein level is similar to that detected for mRNA remains to be further investigated. However, this apparent difference between human and pig healing responses may be indicative of species-species variation in some aspects of the healing process.

In conclusion, an animal model for the study of excisional wound healing has been partially characterized by its wound bacteriology, as well as molecular and cellular biology. This model offers many advantages over small animal models, and because porcine skin is similar to human skin in many respects, results from use of this animal model may be rapidly transferred to human conditions.

Acknowledgments

Support for this research was provided by Westaim Biomedical Corp., Fort Saskatchewan, AB, Canada, and the Canadian Institutes for Health Research. The authors thank Wayne Jansen, Corrie Gallant, Liz Middlemis, Raymond H. Boykiw, Paul Sciore, Linda Marchuk, and Mei Zhang for expert assistance with the studies. JFW is supported by NSERC scholarship, MEO is the Westaim Chair in Biofilm Research, and DAH is the Calgary Foundation-Grace Glaum Professor in Arthritis Research.

References

1. **Davidson, J. M.** 1992. Wound healing, p. 809-819. *In* J. I. Gallin, I. M. Goldstein, and R. Snyderman (ed), Inflammation: basic principles and clinical correlation. Raven Press, Ltd., New York.
2. **Mast, B. A.** 1992. Skin, p. 344-355. *In* I. K. Cohen and W. J. Lindblad (ed.), Wound healing: biochemical and clinical aspects. W. B. Saunders Co., Philadelphia.
3. **Meyer, W., R. Schwartz, and K. Neurand.** 1978. The skin of domestic mammals as a model for the human skin, with special reference to the domestic pig. Curr. Prob. Dermatol.**7:**49-52.
4. **Wang, J. F., M. E. Olson, C. Reno, W. Kulyk, J. B. Wright, and D. A. Hart.** 2000. Molecular and cell biology of skin wound healing in a pig model. Connect. Tissue Res. **41:**195-211.
5. **Lam, K., M. E. Olson, J. B. Wright, and R.E. Burrell.** 1999. Development of a porcine model for examining the influence of wound contamination/infection on wound healing. Wound Rep. Reg. **7:**A305.
6. **Safron, J., and J. C. Gonder.** 1997. The SPF pig in research. ILAR J. **38(1):**28-31.
7. **Reno, C., L. Marchuk., P. Sciore, C. B. Frank, and D. A. Hart.** 1997. Rapid isolation of total RNA from small samples of hypocellular, dense connective tissues. Biotech. **22:**1082-1086.
8. **Schmidt, D. M., and J. D. Ernst.** 1995. A fluorometric assay for the quantification of RNA in solution with nanogram sensitivity. Anal. Biochem. **232:**144-146.
9. **Lipman, J. M.** 1989. Fluorophotometric quantitation of DNA in articular cartilage utilizing Hoechst 33258. Anal. Biochem. **176:**128-131.
10. **Boykiw, R., P. Sciore, C. Reno, L. Marchuk, C. B. Frank, and D. A. Hart.** 1998. Altered levels of extracellular matrix molecule mRNA in healing rabbit ligaments. Matrix. Biol. **17:**371-378.
11. **Majima, T., L. L. Marchuk, P. Sciore, N. G. Shrive, C. B. Frank, and D. A. Hart.** 2000. Compressive compared with tensile loading of medial collateral ligament scar in vitro uniquely influences mRNA levels for aggrecan, collagen type II, and collagenase. J. Orthop. Res. **18:**524-531.
12. **Sciore, P., R. Boykiw, and D. A. Hart.** 1998. Semiquantitative reverse transcription-polymerase chain reaction analysis of mRNA for growth factors and growth factor receptors from normal and healing rabbit medial collateral ligament tissue. J. Orthop. Res.**16:**429-437.
13. **Clifton, D. R., R. A. Goss, S. K. Sahni, R. B. Baggs, V. J. Marder, D. J. Silverman, and L. A. Sporn.** 1998. NF-kappa B-dependent inhibition of apoptosis is essential for host cell survival during *Rickettsia rickettsii* infection. PNAS (USA). **95:**4646-4651.
14. **Brown, D. L., W. Y. K. Winston, and D. G. Greenhalgh.** 1997. Apoptosis down-regulates inflammation under the advancing epithelia wound edge: delayed patterns in diabetes and improvement with topical growth factors. Surgery **121:**372-380.
15. **Kantor, J., and D. J. Margolis.** 1998. Efficacy and prognostic value of simple wound measurements. Arch. Dermatol. **134:**1571-1574.
16. **Rada, J. A., P. K. Cornuet, and J. R. Hassel.** 1993. Regulation of corneal collagen fibrillogenesis in vitro by corneal proteoglycan (lumican and decorin) core proteins. Exp. Eye Res. **56:**635-648.
17. **Mackay, I. A., and I. M. Leigh.** 1991. Epidermal cytokines and their roles in cutaneous wound healing. Br. J. Dermatol. **124:**513-518.
18. **Brigstock, D. R. 1999.** The connective tissue growth factor/cysteine-rich 61/nephroblastoma overexpressed (CCN) family. Endocrine Rev. **20:**89-206.
19. **Brown, D. L., C. D. Kane, S. D. Chernausek, and D. G. Greenhalgh.** 1997. Differential expression and localization of insulin-like growth factors I and II in cutaneous wounds of diabetic and nondiabetic mice. Am. J. Pathol. **151:**715-724.
20. **Ma, S., L. Rao, I. M. Freedberg, and M. Blumenberg.** 1997. Transcriptional control of K5, K6, K14, and K17 keratin genes by AP-1 and NF-kappaB family members. Gene Expr. **6:**361-370.
21. **Waldorf, H., and J. Fawkes** 1995. Wound healing. Adv. Dermatol. **10:**77-96.
22. **Eaglestein, W. H., and V. Falanga.** 1997. Chronic wounds. Surg. Clin. North Am. **77:** 689-700.
23. **Bucknall, T. E.** 1980. The effect of local infection upon wound healing: an experimental study. Br. J. Surg **67:**851-855.
24. **Hats, R. A., R. Niedner, W. Vanscheidt, and W. Westerhof.** 1994. Wound healing and wound management, p. 1-143.24. *In* F. W. Schilderg (ed.). Springer-Verlag GmbH & Co KG, Heidelberg, Germany.
25. **Nicotera, P., M. Leist, and E. Ferrando-May.** 1999. Apoptosis and necrosis: Different execution of the same death. Biochem. Soc. Symp. **66:**69-73.
26. **Desmouliere A., M. Redard, I. Darby, and G. Gabbiani.** 1995. Apoptosis mediates the decrease in cellularity during the transition between granulation tissue and scar. Am. J. Pathol. **146(1):**56-66.
27. **Shrivastava, A., and B. B. Aggarwal.** 1998. Cytokines as biological regulators of homeostasis. J. Biol. Reg. Homeost. Agents **12:**1-24.
28. **Leibovich, S. J., P. J. Polverini, H. M. Shepard, D. M. Wiseman, V. Shively, and N. Nuseir.** 1987. Macrophage-induced angiogenesis is mediated by tumor necrosis factor-alpha. Nature **329:**630-632.
29. **Schreurs, J.** 1993. Cytokines in infectious disease: the battle between host and pathogen. Curr. Opin. Biotechnol. **4:**727-733.
30. **Igarashi, A., H. Okochi, D. M. Bradham, and G. R. Grotendorst.** 1993. Regulation of connective tissue growth factor gene expression in human skin fibroblasts and during wound repair. Mol. Biol. Cell. **4:**637-645.
31. **Frazier, K., S. Williams, D. Kothapalli, H. Klapper, and G. R. Grotendorst.** 1996. Stimulation of fibroblast cell growth, matrix production, and granulation tissue formation by connective tissue growth factor. J. Invest. Dermatol. **107:**404-411.
32. **Grotendorst, G. R., H. Okochi, and Y. Hayashi.** 1996. A novel TGF-β response element controls the expression of connective tissue growth factor gene. Cell Growth Differ. **7:**469-480.
33. **Gartner, M. H., J. D. Benson, and M. D. Caldwell.** 1992. Insulin-like growth factor I and II expression in healing wound. J. Surg. Res. **52:**389-394.
34. **Hart, D. A., N. Nakamura, L. Marchuk, H. Hiraoka, R. Boorman, Y. Kaneda, N. G. Shrive, and C. B. Frank.** 2000. Complexity of determining cause and effect in vivo after antisense gene therapy. Clin. Orthop. **379**(Suppl)**:**S242-S251.
35. **Stander, M., U. Naumann, W. Wick, and M. Weller.** 1999. Transforming growth factor-beta and p-21: multiple molecular targets of decorin-mediated suppression of neoplastic growth. Cell Tissue Res. **296:**221-227.
36. **Kondo, T., Y. Ohshima, and W. Eisenmenger.** 2000. Immunohistochemical study on the expression of c-fos and c-jun in human skin wounds. Histochem. J. **32:**509-514.
37. **Teofoli, P., S. Barduagni, M. Ribuffo, A. Campanella, O. De Pita', and P. Puddu.** 1999. Expression of Bcl-2, p53, c-jun and c-fos protooncogenes in keloids and hypertrophic scars. Dermatol. Sci. **22:**31-37.
38. **Reddy, N. R., B. N. Wilkie, and B. A. Mallard.** 1996. Construction of an internal control to quantitate multiple porcine cytokine mRNAs by RT-PCR. Biotechniques **21(5):**868-875.